Journal of Magnetism and Magnetic Materials 503 (2020) 166622

Contents lists available at ScienceDirect

Journal of Magnetism and Magnetic Materials

journal homepage: www.elsevier.com/locate/jmmm

Research articles

$LaFeO_3$-$CoFe_2O_4$ bi-magnetic composite thin films prepared using an all-in-one synthesis technique

F. Sayed[a], G. Kotnana[a], G. Barucca[b], G. Muscas[c], D. Peddis[d,e], R. Mathieu[a], T. Sarkar[a,*]

[a] Department of Materials Science and Engineering, Uppsala University, Box 534, SE-75121 Uppsala, Sweden
[b] Department SIMAU, University Politecnica delle Marche, Via Brecce Bianche, Ancona 60131, Italy
[c] Department of Physics, University of Cagliari, Cittadella Universitaria di Monserrato, S.P. 8 Km 0.700 (Monserrato-Sestu), I-09042 Monserrato CA, Italy
[d] Dipartimento di Chimica e Chimica Industriale, Università degli Studi di Genova, Via Dodecaneso 31, Genova 16146, Italy
[e] Istituto di Struttura della Materia – CNR, Area della Ricerca di Roma1, Monterotondo Scalo, RM 00015, Italy

ARTICLE INFO

Keywords:
Magnetic oxides
Composite thin films
Chemical solution deposition technique

ABSTRACT

Bi-phasic composite films are generally grown as multilayers that result in layer-by-layer morphology with each layer having a distinct chemical composition. In this work, we report an all-in-one chemical synthesis technique combined with spin-coating to prepare single-layer bi-magnetic $LaFeO_3$ (LFO)-$CoFe_2O_4$ (CFO) composite thin films with both phases co-existing in the same layer. The films have been characterized using X-ray diffraction (XRD) and transmission electron microscopy (TEM), and the magnetic properties have been probed using dc magnetometry at room and low temperature. The unique synthesis technique followed ensures homogeneity of the two phases on the nanoscale with grain sizes ~10 nm for CFO and few tens of nm for LFO, as observed from TEM images. XRD confirms the presence of only the desired LFO and CFO phases in the films without any undesired secondary phases. Magnetic hysteresis loops reveal a coercivity of ~0.2 T at room temperature that increases by nearly one order of magnitude at T = 5 K. The all-in-one synthesis technique reported here can be used to prepare different bi-phasic composites in the form of single-layer two-dimensional films as well as zero-dimensional nanoparticles by a suitable modification of the precursors, solvents, and chelating agents.

1. Introduction

Magnetic composites are important functional materials with potential applications in the development of modern devices [1–6]. In particular, low-dimensional correlated electron oxide systems [7] and their composites [8–10], where the magnetic properties are intricately linked to the structural and electronic properties, offer exciting opportunities [11]. To extend their applicability, these materials need to be grown in the form of thin films using scalable and efficient techniques. In the recent past, we have reported the preparation of prototypical zero-dimensional $LaFeO_3$ (LFO)-$CoFe_2O_4$ (CFO) nanocomposites and demonstrated how the magnetic properties as well as the extent of magnetic coupling in the nanocomposites can be controlled depending on the synthesis route [10]. In this work, we report a unique sol–gel based synthesis technique to prepare bi-phasic thin films of LFO-CFO. The chosen constituent components, LFO and CFO, represent perfect models for two classes of magnetic materials with remarkable physical properties. LFO is a canted G-type antiferromagnet with a high ordering temperature of ~750 K [12]. It has an orthorhombic perovskite structure, in which the Fe^{3+} ion is surrounded by six O^{2-} ions and forms an octahedron. The Fe^{3+} spins are coupled antiferromagnetically with opposite spin direction between two sub-lattices. The second phase in the composite films, CFO, is a typical ferrimagnet (ordering temperature ~800 K) exhibiting high saturation magnetization, high coercivity, and large magnetic anisotropy [13]. Studies that combine LFO with a ferrimagnetic spinel system are relatively rare, although this combination is a promising candidate for tuning the magnetic properties of LFO that can then be used in applications such as sensors, data storage media, spintronic devices, and multiple stage memories [11,14].

The unique “all-in-one” synthesis technique that we use ensures that both phases of the composite film co-exist in the same layer. The samples are, thus, intrinsically different from multilayers or heterostructures [15], where each layer has a distinct chemical composition. In the following sections, we first present the details of the synthesis technique used to prepare the films, followed by their structural, morphological, and magnetic characterization.

* Corresponding author.
E-mail address: tapati.sarkar@angstrom.uu.se (T. Sarkar).

https://doi.org/10.1016/j.jmmm.2020.166622
Received 14 October 2019; Received in revised form 30 January 2020; Accepted 14 February 2020
Available online 15 February 2020

2. Synthesis and experimental techniques

2.1. Synthesis

In a typical synthesis process, individual sols of LFO and CFO were first prepared separately. For the CFO sol, cobalt acetate tetrahydrate $(CH_3COO)_2Co{\cdot}4H_2O$ (Sigma-Aldrich) and iron nitrate nonahydrate $Fe(NO_3)_3{\cdot}9H_2O$ (Sigma-Aldrich) were dissolved at room temperature in stoichiometric amounts in 2-methoxyethanol (Sigma-Aldrich) with a concentration of $[Co^{2+}] = 0.2$ mol.l^{-1}. Next, ethanolamine (EA) was added in a ratio Co^{2+}:Fe^{3+}: EA = 1:2:3. For the LFO sol, stoichiometric amounts of lanthanum nitrate hexahydrate $La(NO_3)_3{\cdot}6H_2O$ (Sigma-Aldrich) and iron nitrate nonahydrate $Fe(NO_3)_3{\cdot}9H_2O$ (Sigma-Aldrich) were dissolved at room temperature in 2-methoxyethanol with a concentration of $[La^{3+}] = 0.2$ mol.l^{-1}. Next, EA was added in a ratio La^{2+}:Fe^{3+}:EA = 1:1:2. The two sols were stirred separately at room temperature using a magnetic stirrer for 1 h to ensure homogeneous mixing of the precursors. Equal volumes of the above sols were then mixed to prepare an LFO/CFO composite sol using a magnetic stirrer for 1 h at room temperature. Mixing equal volumes of the equimolar LFO and CFO sols ensured that the composite sol would lead to a 1:1 ratio of the two phases. LFO, CFO, and LFO/CFO films were prepared by spin-coating the LFO, CFO, and composite sols, respectively, on Si(1 0 0) substrates at 3000 rpm for 30 s. Before deposition, the Si substrates were cleaned using RCA cleaning method followed by oxygen plasma etching. Each film was dried on a hot plate at 200 °C, and then annealed in a muffle furnace at 800 °C for 1 h using a ramping rate of 20 °C/min.

2.2. Characterization techniques

The samples were characterized by X-ray diffraction (XRD) obtained using a D-5000 diffractometer with CuK_α radiation operating at 45 kV and 40 mA. The film was fixed using a specific sample holder at the level of the X-ray source that was fixed at a grazing angle of 1° while the detector scanned the angle range. The data were collected in the range $2\theta = 20 - 80°$, with a step size of 0.05°. Rietveld analysis of the XRD data was performed using MAUD [16].

The composition of the film was investigated by energy dispersive X-ray (EDX) spectroscopy performed using a Tescan Vega3 scanning electron microscope equipped with an EDAX Element microanalysis. The atomic concentrations of La, Co, and Fe were measured on eight different large areas of the sample (each area was approximately 4000 μm^2).

Transmission electron microscopy (TEM) observations were carried out on a Philips CM200 electron microscope equipped with a LaB_6 filament and operating at 200 kV. For TEM cross-sectional observations, samples were prepared by the conventional thinning procedure consisting of mechanical polishing by grinding papers, diamond pastes, and a dimple grinder. Final thinning was carried out by an ion beam system (Gatan PIPS) using Ar ions at 5 kV.

Magnetic field-dependent magnetization of the films was collected using a superconducting quantum interference device (SQUID) magnetometer from Quantum Design Inc. The films were attached on a piece of paper using GE Varnish (Oxford Instruments) and mounted with their planes parallel to the direction of magnetic field. Magnetic hysteresis loops were recorded at T = 300 K and 5 K in the −5 T to +5 T field range.

3. Results and discussion

3.1. Structural and morphological characterization

The XRD patterns of the films are shown in Fig. 1. For the LFO and CFO films, the observed reflections can be indexed to the orthorhombic

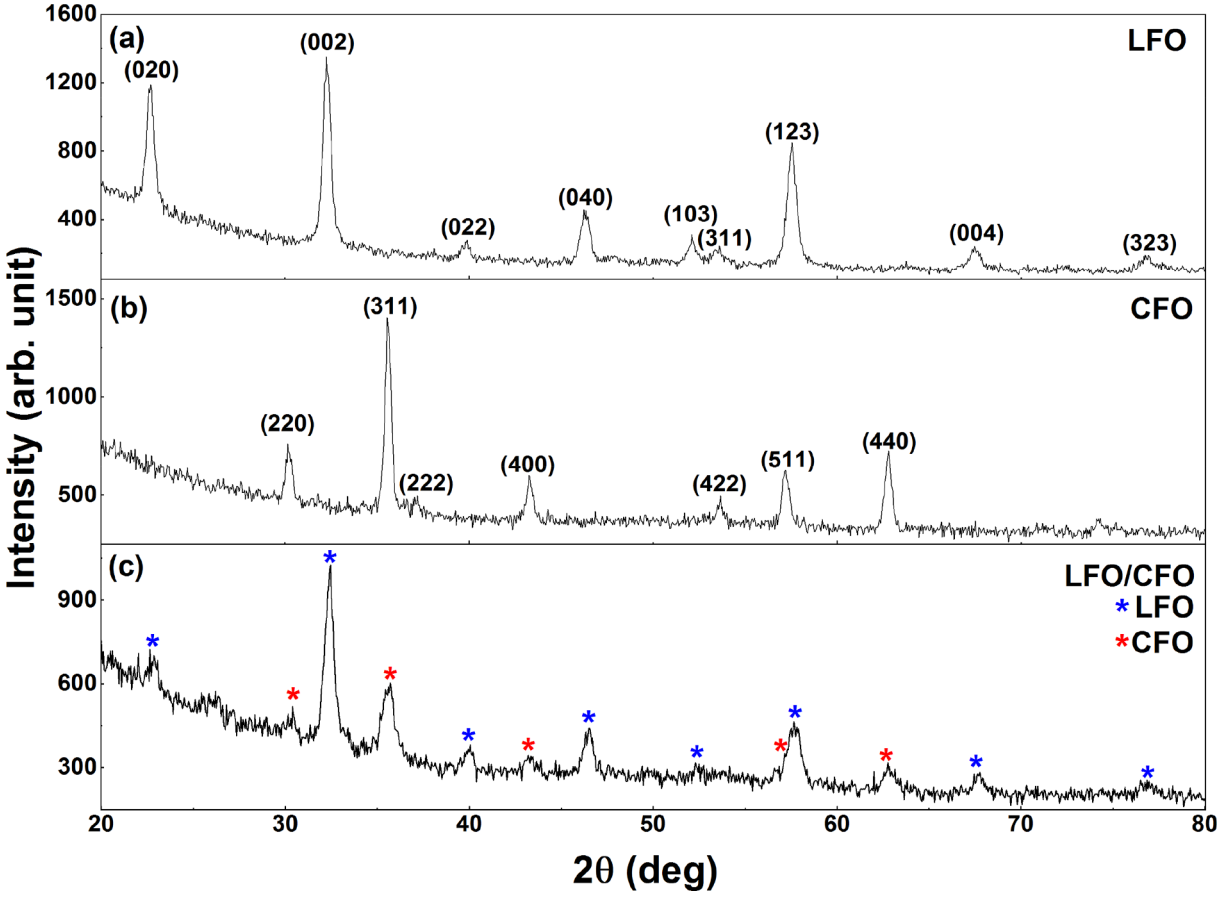

Fig. 1. XRD patterns of (a) LFO, (b) CFO, and (c) LFO/CFO composite thin films.

Table 1
Lattice parameters of the LFO and CFO phases in the LFO, CFO, and composite film as extracted from Rietveld refinement of the XRD data. The lattice parameters corresponding to the reference patterns are also mentioned.

Sample	Phase	Lattice parameters (Å)		
		a	*b*	*c*
LFO film	LFO	5.525(2)	7.853(3)	5.549(2)
CFO film	CFO	8.3625(5)		
LFO/CFO composite film	LFO	5.501(7)	7.837(8)	5.532(6)
	CFO	8.359(2)		
Ref. 258500-ICSD	LFO	5.5621(1)	7.8516(1)	5.5520(1)
Ref. 257981-ICSD	CFO	8.367(1)		

structure of LFO (s.g. *Pnma*) and the cubic structure of CFO (s.g. *Fd-3 m*), respectively, as shown in Fig. 1a and b. For the composite film, reflections corresponding to both LFO and CFO can be observed, as indicated by the blue and red asterisks, respectively in Fig. 1c.

A careful look at the XRD patterns reveals that the reflections corresponding to the LFO phase in the composite film show a right shift of the peaks compared to the pure LFO film. This can be seen more clearly when the XRD patterns are co-plotted on the same graph (Fig. S1 in electronic supplementary material). This shift of the peaks suggests a distortion of the unit cell due to strain. To get a more quantitative measure of the effect of strain on the lattice parameters, we have performed Rietveld refinement of the XRD patterns and extracted the cell parameters. The Rietveld refinement fits are shown in Fig. S2 (electronic supplementary material), and the extracted cell parameters are given in Table 1. The LFO film shows a small decrease in the lattice parameter '*a*' compared to the reference structure (258500-ICSD), while the CFO film has a lattice parameter very close to the bulk reference (257981-ICSD). Analysis of the composite film reveals that the LFO phase undergoes a clear compression of the unit cell will a decrease in all three lattice constants with respect to the bulk, confirming what was qualitatively suggested by the shift of peaks in the XRD pattern.

EDX analysis to check the composition of the composite film yielded the following values in atomic percentage: La = (21 ± 2) At%; Co = (21 ± 2) At%; Fe = (57 ± 2) At%. Oxygen was not considered because EDX technique is not suitable for quantifying light elements. Clearly, the concentration of La and Co is the same and one third of the Fe atomic concentration, inside the experimental errors. This result is in perfect agreement with the nominal composition of the film and the stoichiometry of the compounds: $LaFeO_3$ (50%) + $CoFe_2O_4$ (50%).

TEM analysis was performed on cross sectioned samples. In particular, a general view of the LFO/CFO film is shown in Fig. 2a. The film is composed of superimposed nanocrystals that, in proximity of the substrate, leave space for small pores (red arrows). The nature of the crystals was investigated by selected area electron diffraction (SAED) measurements and high resolution TEM (HR-TEM) observations. Fig. 2b shows a typical diffraction pattern of the film. The biggest spots are due to the silicon substrate, while the other spots can all be attributed to the CFO and LFO phases. HR-TEM analysis has confirmed the crystalline nature of the film, with a general tendency of the LFO phase to be in contact with the substrate and to form larger grains (Fig. 2c). The film thickness is uniform and ~50 nm.

3.2. Magnetization measurements

Field dependence of magnetization of the CFO and LFO/CFO thin films recorded at T = 300 K and 5 K are shown in Fig. 3a and b, respectively. The magnetization values have been corrected for substrate contribution. The LFO film, being antiferromagnetic, has a very low moment that is beyond the measurement capability of the SQUID magnetometer. Fig. 3 shows that the saturation magnetization value of the composite thin film is approximately half the corresponding value of the CFO thin film at both temperatures, in agreement with the ratio of LFO:CFO = 50:50 in the composite thin film. Interestingly, both films show the same value of coercivity (0.2 T) at T = 300 K, while at T = 5 K, the value of coercivity increases marginally in the composite thin film (1.75 T) compared to that of CFO thin film (1.65 T). Such an increase in the coercivity of LFO/CFO compared to the pure phases has been reported before in nanoparticles for certain compositions [17]. The shape of the M(H) loops can be quantified by the parameter $\sigma = M_r/M_{(5T)}$, where M_r = remanent magnetization and $M_{(5T)}$ = magnetization at H = 5 T. The CFO film exhibits a higher value of σ both at low as well as room temperature (σ_{CFO} = 0.66 and 0.40 at T = 5 K and 300 K, respectively, while the corresponding values for the composite film are σ = 0.52 and 0.20). The interface exchange coupling between the antiferromagnetic LFO and ferrimagnetic CFO particles might be responsible for the change in shape of the M(H) loops.

The all-in-one synthesis technique used here, where both phases of the composite film exist in the same layer can lead to unique orientational relationships between the atomic planes of the two phases. We have observed such oriented growth of one phase over the other in nanocomposite samples prepared using a similar synthesis route, where

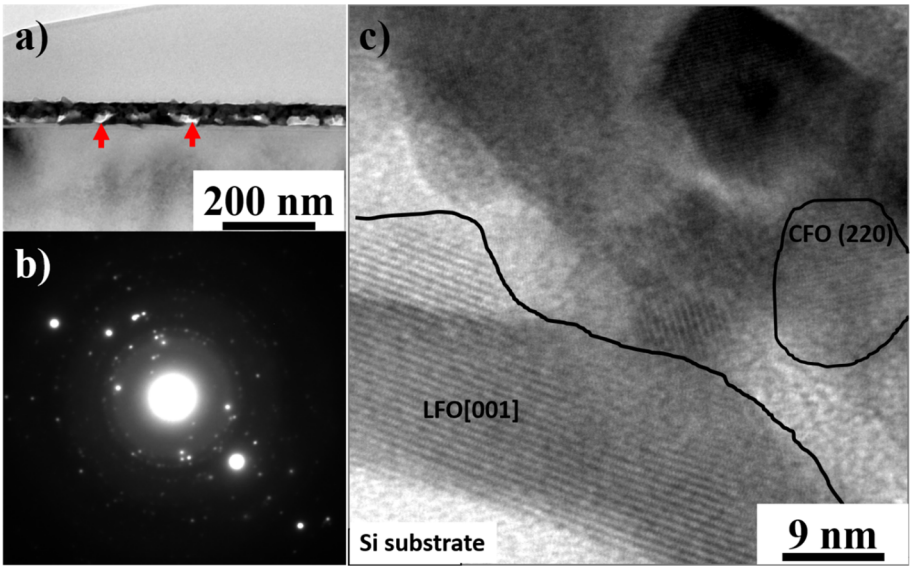

Fig. 2. LFO/CFO composite thin films: a) bright field TEM general view, b) corresponding selected area diffraction pattern, and c) high resolution TEM image.

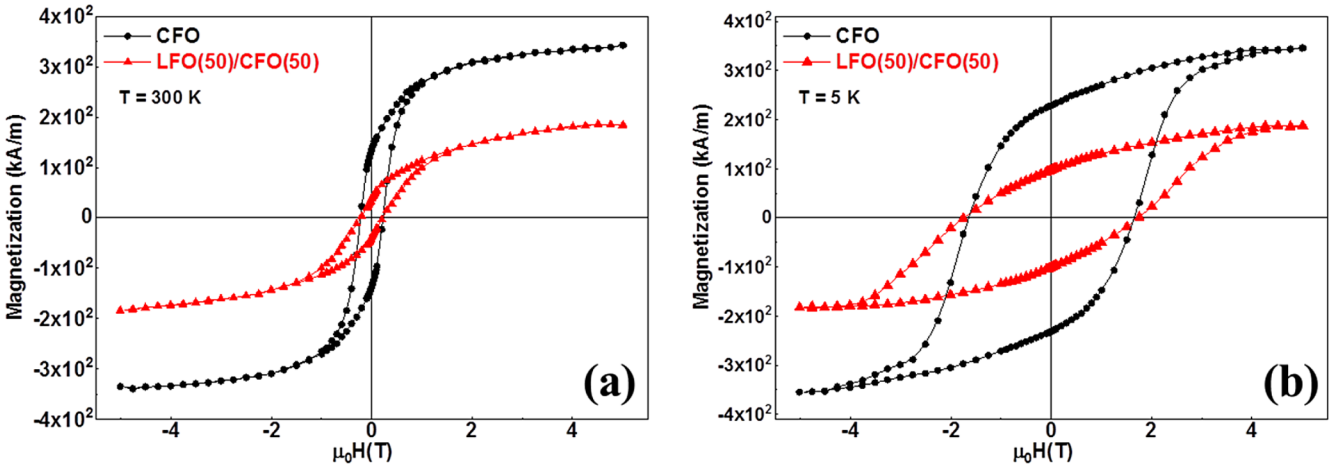

Fig. 3. Isothermal magnetization curves of CFO and LFO/CFO composite thin films at (a) T = 300 K and (b) T = 5 K.

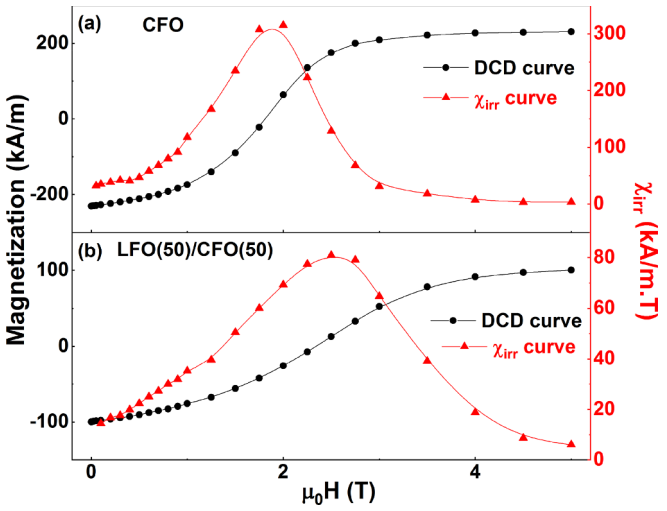

Fig. 4. M_{DCD} versus reverse magnetic field (black curves) and switching field distributions (red curves) of (a) CFO and (b) LFO/CFO composite thin films at T = 5 K.

the atomic planes of one phase were seen to deform in order to match atomic planes of the second phase [18]. Such an interface should lead to very strong magnetic coupling between the two phases. To explore this, we have performed direct current demagnetization (DCD) experiments. In Fig. 4, we show the DCD curves for the CFO and LFO/CFO thin films obtained at T = 5 K. The DCD curve is obtained by first saturating the sample in a negative field (−5 T), and then measuring the remanent magnetization after applying and switching off reverse (positive) fields of increasing amplitude up to H = +5 T. This measurement protocol allows us to investigate the irreversible process of magnetization. Fig. 4 shows the M_{DCD} versus reverse magnetic field (black curves) as well as the differentiated curve of M_{DCD} with respect to H (red curves) for the two films. The latter represents the irreversible component of susceptibility (χ_{irr}). This quantity can be considered to be a measure of the energy barrier distribution, which is associated to the distribution of particle's switching field, defined as the field necessary to overcome the energy barrier during an irreversible process [19]. In general, in a bi-magnetic composite system, when the magnetic coupling between the two phases is weak, the χ_{irr} plots show the presence of two peaks corresponding to the reversal processes of the two individual phases [10]. In this case, however, the χ_{irr} plots show the presence of a single peak, indicating a single average switching field, even for the composite film. This indicates the presence of strong magnetic coupling between the two phases in the composite film, reminiscent of a single-phase material.

4. Conclusions

In summary, we have established a new route to prepare composite thin films with the two phases coexisting in the same layer. Prototypical magnetic systems, antiferromagnetic LFO and ferrimagnetic CFO, were used to demonstrate the new synthesis technique. Our films show a uniform thickness of ~50 nm and grain sizes of ~10 nm for CFO and few tens of nm for LFO. The composite thin film, despite the presence of a large fraction (50%) of an antiferromagnetic phase (LFO) exhibits coercivity values that are comparable to that of CFO both at room as well as low temperatures. This new, low-cost, scalable synthesis technique can be highly useful in preparing composite thin films for applications in different technological areas.

CRediT authorship contribution statement

F. Sayed: Investigation, Validation. **G. Kotnana:** Investigation, Validation. **G. Barucca:** Investigation, Formal analysis, Writing - original draft, Visualization, Writing - review & editing. **G. Muscas:** Formal analysis, Visualization, Writing - review & editing. **D. Peddis:** Writing - review & editing. **R. Mathieu:** Writing - review & editing, Funding acquisition. **T. Sarkar:** Conceptualization, Methodology, Investigation, Validation, Formal analysis, Writing - original draft, Visualization, Writing - review & editing, Supervision, Project administration, Funding acquisition.

Declaration of Competing Interest

The authors declare that they have no known competing financial interests or personal relationships that could have appeared to influence the work reported in this paper.

Acknowledgements

We thank Carl Tryggers Stiftelse för Vetenskaplig Forskning (grant number KF 17:18), Stiftelsen Olle Engkvist Byggmästare (grant number: 188-0179), Swedish Research Council (including VR starting grant number: 2017-05030), and the Royal Physiographic Society of Lund (the Märta and Eric Holmberg Endowment) for financial support. G. Muscas acknowledges financial support from the PON AIM program (Project AIM1809115 - Num. Attività 3 - Linea 2.1).

Appendix A. Supplementary data

Supplementary data to this article can be found online at https://doi.org/10.1016/j.jmmm.2020.166622.

References

[1] M. Li, Y. Wang, A. Chen, A. Naidu, B.S. Napier, W. Li, C.L. Rodriguez, S.A. Crooker, F.G. Omenetto, Flexible magnetic composites for light-controlled actuation and interfaces, PNAS 115 (2018) 8119–8124.

[2] D.W. Lee, A.M. Crawford, S.X. Wang, Composite-anisotropy amorphous magnetic materials for high-frequency devices, J. Appl. Phys. 97 (2005) 10F911.

[3] A. Schoppa, P. Delarbre, Soft magnetic powder composites and potential applications in modern electric machines and devices, IEEE Trans. Magn. 50 (2014) 2004304.

[4] N.H. Abdullah, K. Shameli, E.C. Abdullah, L.C. Abdullah, Solid matrices for fabrication of magnetic iron oxide nanocomposites: synthesis, properties, and application for the adsorption of heavy metal ions and dyes, Compos. B Eng. 162 (2019) 538–568.

[5] L. Zhao, Y. Wang, B. Yang, X. Xu, Y. Yan, M. Huo, X. Wang, and J. Tang, "Magnetic nanocomposite devices for cancer thermochemotherapy", www.intechopen.com, doi: 10.5772/15344.

[6] C. Binns, N. Domingo, A.M. Testa, D. Fiorani, K.N. Trohidou, M. Vasilakaki, J.A. Blackman, A.M. Asaduzzaman, S. Baker, M. Roy, D. Peddis, Interface exchange coupling in Co nanoparticles dispersed in a Mn matrix, J. Phys. Condens. Matter 22 (2010) 436005.

[7] E. Dagotto, Complexity in strongly correlated electronic systems, Science 309 (2005) 257–262.

[8] G. Muscas, P.A. Kumar, G. Barucca, G. Concas, G. Varvaro, R. Mathieu, D. Peddis, Designing new ferrite/manganite nanocomposites, Nanoscale 8 (2016) 2081–2089.

[9] T. Sarkar, G. Muscas, G. Barucca, F. Locardi, G. Varvaro, D. Peddis, R. Mathieu, Tunable single-phase magnetic behavior in chemically synthesized $AFeO_3$-MFe_2O_4 (A = Bi or La, M = Co or Ni) nanocomposites, Nanoscale 10 (2018) 22990–23000.

[10] F. Sayed, G. Muscas, S. Jovanovic, G. Barucca, F. Locardi, G. Varvaro, D. Peddis, R. Mathieu, T. Sarkar, Controlling magnetic coupling in bi-magnetic nanocomposites, Nanoscale 11 (2019) 14256–14265.

[11] M. Bibes, A. Barthélémy, Towards a magnetoelectric memory, Nat. Mater. 7 (2008) 425–426.

[12] W.C. Koehler, E.O. Wollan, Neutron-diffraction study of the magnetic properties of perovskite-like compounds $LaBO_3$, J. Phys. Chem. Solids 2 (1957) 100–106.

[13] G. Muscas, N. Yaacoub, G. Concas, F. Sayed, R. Sayed Hassan, J.M. Greneche, C. Cannas, A. Musinu, V. Foglietti, S. Casciardi, C. Sangregorio, D. Peddis, Evolution of the magnetic structure with chemical composition in spinel iron oxide nanoparticles, Nanoscale 7 (2015) 13576–13585.

[14] J.F. Scott, Multiferroic memories, Nat. Mater. 6 (2007) 256–257.

[15] Y. Bai, J. Chen, S. Zhao, Q. Lu, Magneto-dielectric and magnetoelectric anisotropies of $CoFe_2O_4/Bi_5Ti_3FeO_{15}$ bilayer composite heterostructural films, RSC Adv. 6 (2016) 52353–52359.

[16] L. Lutterotti, S. Matthies, H.R. Wenk, International Union of Crystallography Newsletter 21 (1999) 14–15.

[17] E.E. Ateia, M.K. Abdelamksoud, M.A. Rizk, Improvement of the physical properties of novel (1–x) CoFe2O4 + (x) LaFeO3 nanocompsoites for technological applications, J. Mater. Sci: Mater. Electron. 28 (2017) 16547–16553.

[18] F. Sayed, G. Kotnana, G. Muscas, F. Locardi, A. Comite, G. Varvaro, D. Peddis, G. Barucca, R. Mathieu, T. Sarkar, Symbiotic, low-temperature, and scalable synthesis of bi-magnetic complex oxide nanocomposites, Nanoscale Adv. 2 (2020) 851–859.

[19] D. Peddis, P.E. Jönsson, S. Laureti, G. Varvaro, Magnetic interactions: a tool to modify the magnetic properties of materials based on nanoparticles, Frontiers of Nanoscience 6 (2014) 129–188.